

Molecular Dynamics Simulation of Folding and Diffusion of Proteins in Nanopores

Leili Javidpour,^a Muhammad Sahimi,^{b,†} and M. Reza Rahimi Tabar^{a,c}

^a Dep. of Physics, Sharif University of Technology, Tehran 11365, Iran

^b Mork Family Department of Chemical Engineering & Materials Science, University of Southern California, Los Angeles, California 90089-1211, USA

^c CNRS UMR 6529, Observatoire de la Côte d'Azur, BP 4229, 06304 Nice Cedex 4, France

A novel combination of discontinuous molecular dynamics and the Langevin equation, together with an intermediate-resolution model, are used to carry out long (several μ s) simulation and study the stability, folding transition, and diffusion of proteins in nanopores. With an attractive potential U^+ between the proteins and the pore's walls, the folding temperature T_f decreases with decreasing pore sizes, but the opposite is true when the potential is repulsive. Near T_f and in the presence of U^+ the proteins undergo a repeating sequence of folding/partially-folding/unfolding transitions. Also computed are the proteins' diffusivity and its dependence on the temperature, the pore's size, and proteins' length (number of amino acid groups).

PACS: 87.15.Aa, 83.10.Mj, 87.15.Cc, 87.15.Vv, 87.83.+a

Proteins' importance to biological systems cannot be overstated [1]: as enzymes they catalyze and regulate cells' activities; tissues are made of proteins, while as antibodies proteins are a vital part of the immune system. Proteins with globular structure fold into compact and biologically active configurations, and an important problem is understanding the mechanisms by which they attain their folded structure, and factors that contribute to the folding [2]. Such understanding is important due to debilitating illnesses that afflict people, such as Alzheimer's and Parkinson's diseases, that are believed to be the result of accumulation of toxic protein aggregates [3-5], as well as to the industrial production of enzymes and therapeutic proteins based on the DNA recombinant method [6].

While the three-dimensional (3D) structure of native proteins is controlled by their amino acid sequence [2], their transport properties and the kinetics of their folding depend on the local environment. But, whereas protein folding in dilute solutions under bulk condition, typically used in *in vitro* studies, is relatively well-understood, the same but more important problem in a confined medium is not. The environment inside a cell in which proteins fold is crowded, with the volume fraction of the crowding agents (such as RNA) may be 0.2-0.3. Thus, even in the absence of interactions between proteins and other cellular molecules, their movement inside the cell is limited. The limitation affects proteins' stability. Experiments indicated [7] that confinement often stabilizes the proteins' native structure, [8] denatures them in the limited space of the cage model, first suggested by Anfinsen [2], and *accelerates* folding relative to that in bulk solutions. Studies of proteins of different native architectures in cylindrical nanopores indicated [9] that, *in vivo* folding is *not* always spontaneous; rather, a subset of proteins may require molecular chaperones.

Protein (enzyme) immobilization using porous solid

support, via adsorption, encapsulation, and covalent linking, has been used for a long time [10]. Such practical applications as biocatalysis [11] and biosensors also entail better understanding of the folding in confined media. Protein purification using nanoporous membranes is also gaining attention [12]. SiC nanoporous membranes [13] allow [14] diffusion of proteins up to 29000 Daltons, but exclude larger ones.

In this Letter we use a novel combination of molecular dynamics (MD) simulation and the Langevin dynamics to study protein folding, stability, and diffusion in nanopores. A nanopore is a reasonable model for the pores that one encounters in biocatalysts, sensors, and membranes [11-14]. Some Monte Carlo [15] and MD [16] simulations of proteins' behavior in nanopores have been reported before. But, to our knowledge, simulation of diffusion of proteins in nanopores, as well as several other aspects of our study, such as utilizing the detailed protein model that we use, have not been undertaken before.

We simulate *de novo*-designed α family of proteins [17], which consists of only 4 types of amino acids in their 16-residue sequence, simplified further [18] to a sequence of hydrophobic (H) and polar (P) residues. Using periodicity in the H-P sequence of the 16-residue peptide α_{1B} , we made 3 other sequences with lengths $\ell = 9, 23$ and 30 residues. As the four proteins have similar native structures, the differences in their behavior is attributed to their lengths. The simulations indicated that they all fold into an α -helix.

The proteins are modeled by an intermediate-resolution model [19,20], with several changes described below. Every amino acid is represented by four united atom (UA) groups or beads. A nitrogen UA represents the amide N and hydrogen of an amino acid, a C_α UA represents the α -C and its H, and a C UA the carbonyl C and O. The fourth bead R represents the side chains, all of which are assumed to have the same diameter as CH_3 .

All the backbone bond lengths and bond angles are fixed at their ideal values, and the distance between consecutive C_α UAs is fixed according to experimental data.

To carry out long and efficient simulations, we use discontinuous MD (DMD) [21]. The forces acting on the beads are the excluded-volume effect, and attraction between bonded and pseudobonded beads, between pairs of backbone beads during HB formation, and between hydrophobic side chains. Nearest-neighbor beads along the chain backbone are covalently bonded, as are the C_α and R UAs. Pseudobonds are between next-nearest neighbor beads along the backbone to keep the backbone angles fixed; between neighboring pairs of C_α beads to maintain their distances close to the experimental data, and between side chains and backbone N and C UAs to hold the side-chain beads fixed relative to the backbone. All of this keep the interpeptide group in the *trans* configuration, and all the residues as *L*-isomers, as required.

The potential U_{ij} between a pair ij of bonded beads, separated by a distance r_{ij} , is given by, $U_{ij} = \infty$, for, $r_{ij} \leq l(1 - \delta)$, and $r_{ij} \geq l(1 + \delta)$, and, $U_{ij} = 0$ for $l(1 - \delta) < r_{ij} < l(1 + \delta)$. Here, l is the ideal bond length, and $\delta = 0.02375$ is the tolerance in the bond's length [19,20]. The hydrophobic (HP) interactions between the side chains and the H in the sequence, if there are at least 3 intervening residues between them, is given by, $U_{\text{HP}} = \infty$, $-\epsilon_{\text{HP}}$, and 0 for, $r_{ij} \leq \sigma_{\text{HP}}$, $\sigma_{\text{HP}} < r_{ij} \leq 1.5\sigma_{\text{HP}}$, and $r_{ij} > 1.5\sigma_{\text{HP}}$, respectively, where σ_{HP} is the HP side-chains' diameter.

The HB interaction may occur between the N and C beads with at least 3 intervening residues, but each bead may not contribute to more than one HB at any time, with the range of the interaction being about 4.2 Å. The HBs are stable when the angles in N-H-O and C-O-H, controlled by a repulsive interaction between each of the N and C beads with the neighboring beads of the other one, are almost 180°. Thus, if a HB is formed between beads N_i and C_j , a repulsive interaction between neighbor beads of N_i , namely, C_{i-1} and $C_{\alpha i}$, with C_j is assumed, and similarly for the neighbor beads of C_j , namely, N_{j+1} and $C_{\alpha j}$, with the N_i bead.

An N or C bead at one end of the protein has only one neighbor bead in its backbone, instead of 2. Hence, controlling the HB angles will be limited, causing the HBs with one of their terminal constituents to be less restricted and, thus, more stable than the other HBs. This may cause formation of non- α -helical HBs in a part of the protein between the N and C beads, and of semistable structures that influence the results. To address this problem, assume that the N-terminal bead, N_1 , has a HB with C_j . For $i = 1$, bead C_{i-1} does not exist to have a repulsive interaction with C_j and help control the HB angles. So, we use $C_{\alpha 1}$. Not only can we consider the repulsion between this bead and C_j , but also we define an upper limit for their distance so as to control the motion freedom of N_1 and C_j that constitute the

beads in the HB. The potential U_{kl} of such interactions is given by, $U_{kl} = \infty$, ϵ_{HB} , 0, and ∞ for $r_{kl} \leq \frac{1}{2}(\sigma_k + \sigma_l)$, $\frac{1}{2}(\sigma_k + \sigma_l) < r_{kl} \leq d_1$, $d_1 < r_{kl} \leq d_2$, and, $r_{kl} > d_2$, respectively.

Two H atoms have chemical bonds with the nitrogen in the proteins' N-terminal, and are free to rotate around the $N_1-C_{\alpha 1}$ bond, while at the same time satisfying the constraints on the angles between the chemical bonds of N_1 . Thus, if a HB is formed, one of the two H atoms lies in the plane of N, O and C, such that the angles in N-H-O and C-O-H are as close to 180° as possible. Hence, we force the maximum distance between $C_{\alpha 1}$ and C_j to be the same as the maximum distance d_2 between $C_{\alpha i}$ and C_j in the usual HBs, and similarly when the C-terminal C_ℓ has a HB with N_i . This allows us to control the angles in a HB that contains N_1 . The T -dependence (T is dimensionless) of d_2 (in Å), obtained from separate simulations (the details will be given elsewhere), is, $d_2 \simeq 5.53 - 0.019/T$ for $N_1-C_{\alpha j}$, and $d_2 \simeq 5.69 - 0.044/T$ for $C_\ell-C_{\alpha i}$.

There is also hard-core repulsion between two unbonded beads that have no HB and HP interactions. At the same time, interactions between a pair of beads, separated along the chain by 3 or fewer bonds, are more accurately represented by those between the atoms themselves, not the UAs. Thus, we develop a variant of the previous models [19,20] to account for such interactions: the beads are allowed to overlap by up to 25% of their bead diameters, while for those separated by 4 bead diameters the allowed overlap is 15% of their diameters.

We use a slit nanopore, modeled as the space between two 2D structureless carbon walls in the xy plane between $z = \pm h/2$, with periodic boundary conditions in the x and y directions. The interaction between the walls and the protein beads is, $U_{\text{PW}} = \infty$, ϵ_{PW} , 0, ϵ_{PW} , and ∞ for, $z_X \leq -(h/2 - d_{3X})$, $-(h/2 - d_{3X}) < z_X \leq -(h/2 - d_{3X} - d_{4X})$, $-(h/2 - d_{3X} - d_{4X}) < z_X \leq h/2 - d_{3X} - d_{4X}$, $h/2 - d_{3X} - d_{4X} < z_X \leq h/2 - d_{3X}$, and $z_X \geq h/2 - d_{3X}$, respectively, where z_X is the distance between the center of a bead X and the walls. For all the beads, $\epsilon_{\text{PW}} = \epsilon_{\text{HB}}/8$, so chosen to represent realistically the competition between protein folding and its beads' interaction with the walls. To estimate d_{3X} and d_{4X} , the energy and size parameters between the C atoms in the walls and various beads were calculated using Lorentz-Berthelot mixing rules, $\sigma_{CX} = \frac{1}{2}(\sigma_C + \sigma_X)$, and $\epsilon_{CX} = \sqrt{\epsilon_C \epsilon_X}$, where $X = \text{N, } C_\alpha, \text{C and R}$. Then, using separate simulations (details will be given elsewhere), the interaction potential U_{CX} between different beads was estimated. The distances at which U_{CX} and its second derivative were zero were taken as d_{3X} and $d_{3X} + d_{4X}$. The results (in Å) are, $d_{3X} = 2.85, 3.02, 3.14$, and 3.31 , and $d_{4X} = 0.96, 1.01, 0.98$, and 1.12 , for $X = \text{N, } C_\alpha, \text{C, and R}$, respectively.

In the previous works the the effect of the solvent was included implicitly by the HP attraction between

the side chains. While this might be appropriate for studying the folding, it is not so for computing the proteins' diffusion coefficient. To explicitly include the solvent effect, we first carry out DMD simulation for a time Δt . The speed of the proteins' center of mass (CM) at the beginning of the period is \mathbf{v}_b and at the end is \mathbf{v}_e . We then apply the Langevin equation (LE) to the CM to correct the proteins' velocity due to the presence of the solvent's molecules. Representing a protein as a spherical particle with mass m and radius equal to its radius of gyration R_g , the force \mathbf{F} on its CM is given by, $\mathbf{F} = m(\mathbf{v}_e - \mathbf{v}_b)/\Delta t$. The discretized LE is, $\Delta \mathbf{v} = \mathbf{v}_n - \mathbf{v}_b = \mathbf{F}\Delta t/m - \xi \mathbf{v}_b \Delta t/m + \Delta \mathbf{R}(\Delta t)$, where, $\xi = 6\pi R_g \eta$, $\Delta \mathbf{R}$ is a Gaussian random force (with zero mean and variance $2k_B T \xi \Delta t / m^2$), and \mathbf{v}_n is the speed *after* applying the LE (acting as the \mathbf{v}_b for the next LE application). Thus, $d\mathbf{v} = \mathbf{v}_n - \mathbf{v}_e = -\xi \Delta t \mathbf{v}_b / m + \Delta \mathbf{R}(\Delta t)$, which corrects the protein's velocity due to the presence of the solvent. The DMD simulation is then continued for a time Δt , the LE is applied again, and so on.

Consider the case of attractive interaction potential U^+ between the proteins and the pore's walls. A folded state attaches itself to the walls only through its end groups, while unfolded ones may completely attach themselves to the walls. Thus, with U^+ the decrease in the average potential energy of the unfolded states is larger than the corresponding decrease for the folded one. Hence, compared to the bulk, the unfolded states in the pore with a U^+ are more stable than the folded one. Figure 1 shows a sequence of events for a protein of size $\ell = 16$ in a pore of size $h = 1.75$ nm at $T_f \simeq 0.13$. The protein changes its state from completely folded to a partially folded to an unfolded one which is completely attached to the pore's wall (frame D). Due to U^+ , the transitions occur easily and repeatedly, even after a long time. Note that, in moving from frame B to C, the set of deformed α -helical HBs changes, hence indicating rapid dynamics of the HB formation and deformation near T_f .

But, with a purely repulsive interaction U^- between the walls and the proteins, they will be even more confined. Thus, the number of possible unfolded states and, hence, their total entropy, will be smaller [22]. But, due to its compact configuration, confinement affects the entropy of the folded state less strongly. This implies that, with U^- the folded state is more stable than that in the bulk.

Figure 2 presents the average interaction energy $\langle U_{PW} \rangle$ of the proteins with the walls, and $\langle n_\alpha \rangle$, the average number of the α -helical HBs, computed by the weighted histogram analysis method [23]. Cooling the proteins at $T > T_f$ increases $|\langle U_{PW} \rangle|$, as well as $\langle n_\alpha \rangle$ which is, however, very small. Near T_f , where the protein begins to have a nonnegligible $\langle n_\alpha \rangle$ and α -helical structure starts to appear, the proteins can only laterally attach themselves to the walls, hence decreasing $|\langle U_{PW} \rangle|$. By lowering T further, nearly the entire α -helix is formed, and

$|\langle U_{PW} \rangle|$ increases again. This indicates that, not only does the interaction with a nanopore disturb folding (see above), but also folding to a definite structure disturbs the proteins' interaction with the pore.

Figure 3 presents T_f as a function of the pore and protein sizes, computed as the maximum in a plot of the heat capacity C_v versus T [23]. That T_f decreases with the pore size is due to the attractive interaction energy between the protein and the walls. The opposite is true if the interaction is purely repulsive. The decrease in T_f is indicative of the more stable unfolded states (or less stable folded state). However, in the two smallest pores, a protein of length $\ell = 9$ does not attain its native state at low T . Instead, it has a U shape, with its two sides attached to the walls, has 4 HBs, only one of which is α -helical (the native state has 5 α -helical HBs), and more of its atoms are close to the walls than those in the folded state. Although the potential energy of this unfolded state is roughly the same as one in the folded one, entropic effects, that favor the unfolded state, are also important. In this case, we do not consider the maximum in the C_v plot as a true T_f because, upon further cooling at T below this temperature, the protein becomes trapped in the U shape without enough kinetic energy to overcome the energy barrier to attain a folded state, whereas, normally, the protein should attain its native state at such temperatures.

Figure 4 presents the diffusion coefficient D of the proteins, both in the bulk and in the pores (in the xy planes parallel to the walls). As T increases, so also does D . In all cases, far from T_f (where R_g changes little) D varies roughly linearly with T . However, near T_f , R_g strongly varies with T and, consequently, D no longer varies linearly with T . Increasing the proteins' size or decreasing the pore's size decreases the diffusivity, as expected.

We thank M. R. Ejtehadi, C. K. Hall, and M. D. Niry for useful discussions. The work of LJ was supported by Iranian Nanotechnology Initiative.

- [1] C. Branden and J. Tooze, *Introduction to Protein Structure*, 2nd ed. (Garland Publishing, New York, 1998).
- [2] C. B. Anfinsen, *Science* **181**, 223 (1973); D. K. Klimov and D. Thirumalai, *Phys. Rev. Lett.* **76**, 4070 (1996); L. Mirny and E. Shakhnovich, *Annu. Rev. Biophys. Biomol. Struct.* **30**, 361 (2001).
- [3] S. Lu, Z. Liu, and J. Wu, *Biophys. J. BioFAST* **105**, 071761 (2006).
- [4] D. A. Kirschner, C. Abraham, and D. J. Selkoe, *Proc. Natl. Acad. Sci. USA* **83**, 503 (1986); K. A. Conway, *et al.*, *ibid.* **97**, 571 (2000).
- [5] D. G. Lynn and S. C. Meredith, *J. Struct. Biol.* **130**, 153 (2000).

- [6] J. G. Thomas, A. Ayling, and F. Baneyx, *Appl. Biochem. Biotechnol.* **66**, 197 (1997).
- [7] D. K. Eggers and J. S. Valentine, *Prot. Sci.* **10**, 250 (2001).
- [8] A. Brinker, *et al.* *Cell* **107**, 223 (2001).
- [9] F. Tagaki, N. Koga, and S. Takada, *Proc. Natl. Acad. Sci. USA* **100**, 11367 (2003).
- [10] *Immobilization of Enzymes and Cells*, edited by G. F. Bickerstaff (Humana Press, Totowa, NJ, 1997); C. Lei, *et al.*, *J. Am. Chem. Soc.* **124**, 11242 (2002).
- [11] M. Dadvar and M. Sahimi, *Chem. Eng. Sci.* **58**, 4935 (2003).
- [12] M.-E. Avramescu, Z. Borneman, and M. Wessling, *Biotechnol. Bioeng.* **84**, 564 (2003).
- [13] A. J. Rosenbloom, *et al.*, *Biomed. Microdev.* **6**, 261 (2004).
- [14] B. Elyassi, M. Sahimi, and T. T. Tsotsis, *J. Memb. Sci.* **288**, 290 (2007).
- [15] G. Ping, *et al.*, *J. Chem. Phys.* **118**, 8042 (2003).
- [16] M. S. Cheung, D. Klimov, and D. Thirumalai, *Proc. Natl. Acad. Sci. USA* **102**, 4753 (2005).
- [17] L. Regan and W. F. DeGrado, *Science* **241**, 976 (1988).
- [18] Z. Guo and D. Thirumalai, *J. Mol. Biol.* **263**, 323 (1996).
- [19] S. Takada, Z. Luthey-Schulten, and P. G. Wolynes, *J. Chem. Phys.* **110**, 11616 (1999).
- [20] A. V. Smith and C. K. Hall, *Proteins* **44**, 344, 376 (2001); H. D. Nguyen, A. J. Marchut and C. K. Hall, *Prot. Sci.* **13**, 2909 (2004).
- [21] S. W. Smith, C. K. Hall, and B. D. Freeman, *J. Comput. Phys.* **134**, 16 (1997).
- [22] D. Thirumalai, D. K. Klimov, and G. H. Lorimer, *Proc. Natl. Acad. Sci. USA* **100**, 11195 (2003).
- [23] A. M. Ferrenberg and R. H. Swendsen, *Phys. Rev. Lett.* **63**, 1195 (1989).

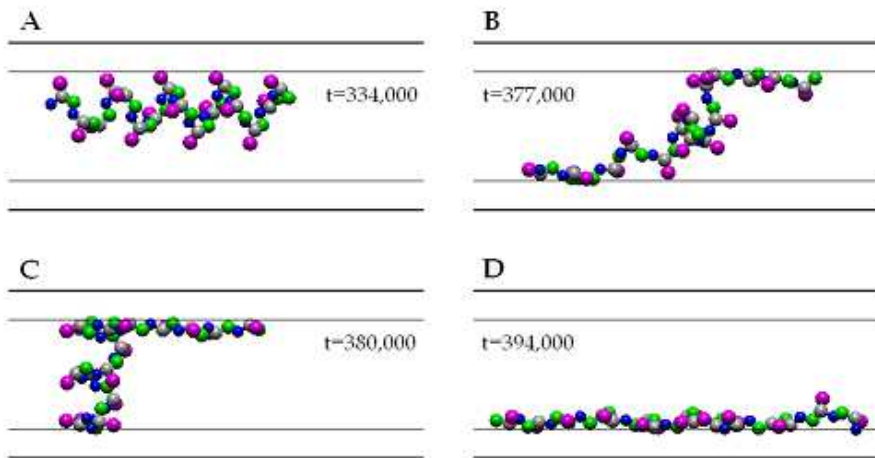


FIG. 1. A protein of length $\ell = 16$ at $T_f \simeq 0.13$. Blue, gray, green, and pink spheres show, respectively, the N bead, C_α , C, and the side chains. In between the walls and the thin lines at a distance d_3 , $U_{PW} = \infty$, beyond which the U^+ acts for a distance d_4 .

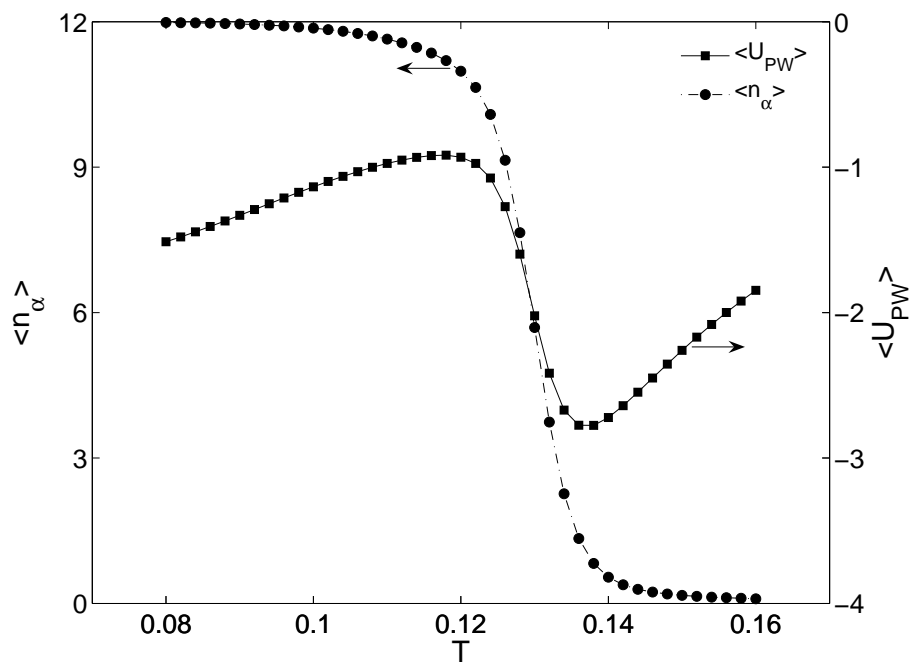


FIG. 2. The average interaction energy $\langle U_{PW} \rangle$ and number of α -helical HBs $\langle n_\alpha \rangle$.

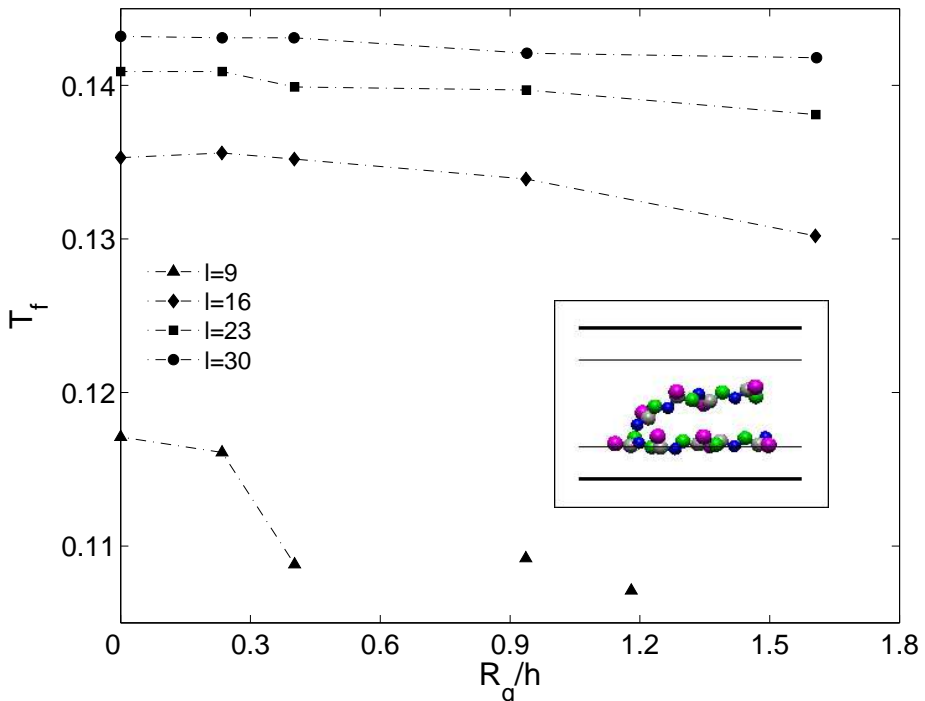


FIG. 3. Folding temperatures T_f for proteins of size ℓ and pore sizes h . The radius of gyration R_g is constant, computed at $T = 0.08$ under bulk condition ($R_g/h = 0$). The two unconnected cases for $\ell = 9$ do not attain their native state, with the inset showing their conformation.

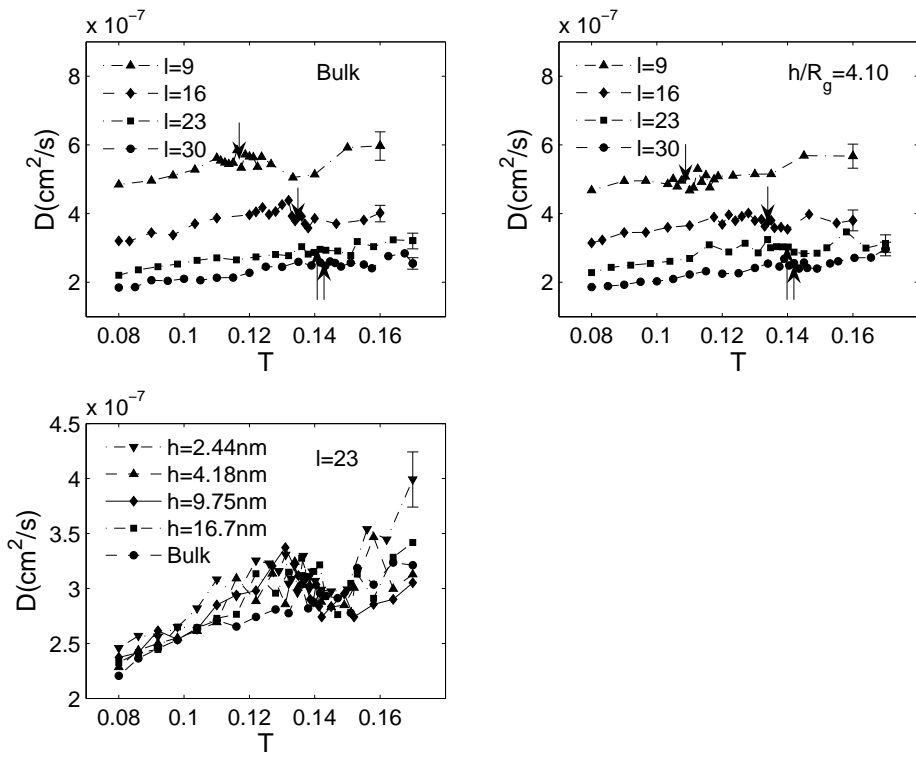


FIG. 4. The diffusion coefficients D in the pores and under bulk condition. Arrows indicate the location of T_f .